

Self-Similarity and Universality in Rayleigh-Taylor, Boussinesq Turbulence

Natalia Vladimirova*

ASC Flash Center, The University of Chicago, Chicago, IL 60637[†]

Michael Chertkov[‡]

CNLS and T-13, Theory Division, Los Alamos National Laboratory, Los Alamos, NM 87544

We report and discuss case study simulations of the Rayleigh-Taylor instability in the Boussinesq, incompressible regime developed to turbulence. Our main focus is on a statistical analysis of temperature and velocity fluctuations inside of the already developed and growing in size mixing zone. Novel observations reported in the manuscript concern self-similarity of the velocity and density fluctuations spectra inside of the mixing zone snapshot, independence of the spectra of the horizontal slice level, and universality showing itself in a virtual independence of the internal structure of the mixing zone, measured in the re-scaled spatial units, of the initial interface perturbations.

Keywords: turbulence — mixing zone — scale-separation — self-similarity — universality

The Rayleigh-Taylor instability occurs when a heavy fluid is being pushed by a light fluid. Two plane-parallel layers of fluid, colder on a top, are in equilibrium, but the slightest perturbation leads to the denser material moving down under the gravitational field, and the lighter material being displaced upwards. The early, linear stage of the instability was described by Rayleigh [1] and Taylor [2], and summarized in [3]. Further development of the instability leads to enhancement of the mixing and to a gradual increase of the mixing zone, which is the domain where proportions of heavy in light and light in heavy are comparable. Dimensional arguments, supported by large-scale modeling [4, 5], suggest that the half-width of the mixing zone, h , grows quadratically at the later time, $h \propto \alpha A g t^2$, where A is the Atwood number characterizing the initial density contrast, g is the gravity acceleration, and α is a dimensionless coefficient.

The coefficient α was the focus of almost any paper written on the subject of Rayleigh-Taylor turbulence (RTT) in the course of the last fifty years. The results of many studies and controversies surrounding the α -coefficient was recently summarized in the review combining and analyzing the majority of existing α -testing simulations and experiments [6]. In this manuscript we also discuss the developed regime of RT turbulence; however our main focus is on the analysis of the internal structure of the mixing zone. The α -coefficient is traced only for validation purposes.

Our analysis of the external structure of the mixing zone develops and extends previous experimental [7, 8] and numerical [7, 9, 10, 11, 12] observations on the subject. It is also guided by phenomenological considerations discussed in [13]. The essence of the phe-

nomenology, which utilizes the classical Kolmogorov-41 [14] approach, can be summarized in the following statements. (i) The mixing zone width, h , and the energy containing scale, R_0 , are well separated from the viscous, η , and diffusive, r_d , scales. In the inertial range, realized in the asymptotically large range bounded by R_0/η from above/below, the turbulence is adiabatically adjusted to the large-scale buoyancy-controlled dynamics. (ii) In three dimensions, the velocity fluctuations at smaller scales are asymptotically decoupled from weaker buoyancy effects[20]. (iii) Typical values of velocity and density fluctuations scale the same way as in the stationary, homogeneous Kolmogorov turbulence, $\delta v_r \sim (\epsilon r)^{1/3}$, and $\delta \rho_r \sim \epsilon_r^{1/2} \epsilon^{-1/6} r^{1/3}$, where the energy Kolmogorov flux, ϵ , increases with time while the density fluctuations flux, ϵ_r , remains constant, according to the buoyancy prescribed large scale dynamics. All of these three theses of the phenomenology are consistent with available experimental [7, 8] and numerical [9, 10, 12, 16] observations of the velocity and density spectra. Besides, one, particularly important, consequence of the phenomenology, the decrease of the viscous and dissipative scales, was also predicted in [11] and numerically confirmed in [11, 12].

In spite on its relative success in explaining RTT, the phenomenology [13] is, obviously, not free from deficiencies. First, the asymptotic large time character of the phenomenology becomes a handicap in explaining numerical and experimental data, taken at finite, and actually modest, times. Second, the phenomenology treats all z -slices within the mixing zone equally. Third, the phenomenology does not differentiate between the mixing zone width, h , and the energy containing scale, R_0 , for the turbulent fluctuations.

Improving the phenomenology from within itself, or by some complementary theoretical means, does not seem feasible, and one can only rely on resolving questions/uncertainties through experiments and simulations. This manuscript reports a step in this direction. Here we raise and give partial answers, based on simula-

*Electronic address: nata@flash.uchicago.edu

[†]also at CNLS and T-13, Theory Division, Los Alamos National Laboratory, Los Alamos, NM 87544

[‡]Electronic address: chertkov@lanl.gov

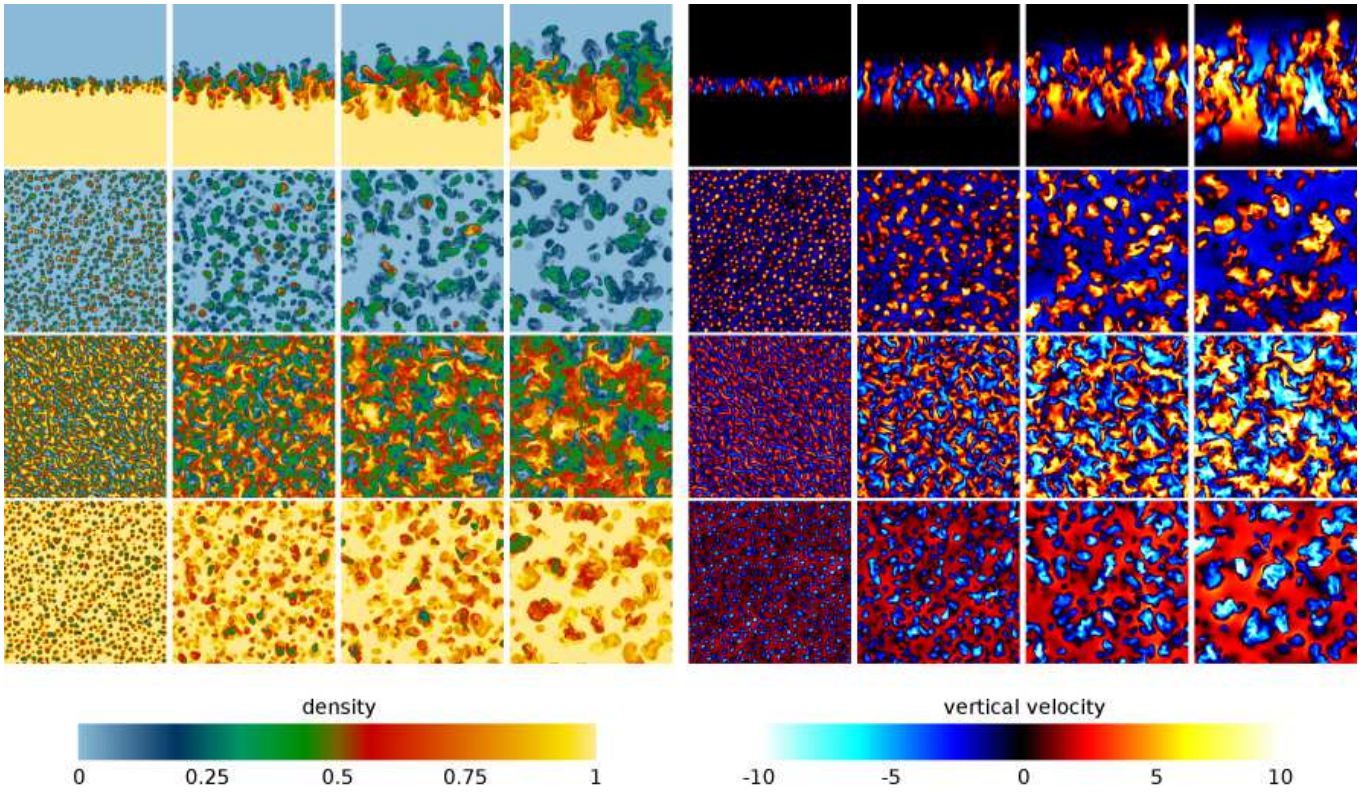


FIG. 1: Slices of density and vertical velocity at times $t = 32, 64, 96, 128$ (left to right) in simulation with narrow initial spectrum in 960^3 domain; from top to bottom, the images correspond to vertical slice at $y = 480$ and horizontal slices at $z = +0.75h, 0, -0.75h$.

tions, to the following subset of key questions concerning the internal structure of the RTT mixing zone:

- Analyzing the evolution of h , R_0 , r_d and η with time one often observes a non-universal, simulation/experiment specific behavior, especially at transient, so-called early self-similarity, times [11]. Will the relative dependence of scales be a more reliable indicator of a universal behavior than the time-dependence of the scales?
- How does the energy containing scale, R_0 , compare with the width of the mixing layer, h ? This question was already addressed in [11]. Here, we will elaborate on this point.
- How different are the turbulent spectra at different vertical positions in the mixing zone within a given time snapshot?
- How different are the scales and spectra corresponding to qualitatively different initial perturbations?

The material in this manuscript is organized as follows. We start by describing our simulations, and proceed to definitions and subsequently observations of the various

spatial scales characterizing a time snapshot of the mixing zone. Finally we turn to discussing self-similarity and universality of the emerging spatio-temporal picture of the RTT. We conclude by answering the questions posed above.

I. DESCRIPTION OF SIMULATIONS

We consider 3D incompressible, miscible Rayleigh-Taylor flow in the Boussinesq regime,

$$\partial_t \mathbf{v} + (\mathbf{v} \cdot \nabla) \mathbf{v} + \nabla p - \nu \Delta \mathbf{v} = -Agc, \quad \nabla \cdot \mathbf{v} = 0, \quad (1)$$

$$\partial_t c + (\mathbf{v} \cdot \nabla) c = \kappa \Delta c, \quad (2)$$

where κ and ν are the diffusion and viscosity coefficients, while $c = (\rho - \rho_{\min})/(\rho_{\max} - \rho_{\min})$ is the normalized density. The Boussinesq approximation for gravity describes fluids with small density contrast, $A \ll 1$. Here, we restrict ourselves to the case of $\kappa = \nu$.

We solve equations (1-2) using the spectral element code developed by Fischer et al [18]. The equations are solved in the nondimensional units,

$$[l] = (2Ag)^{-\frac{1}{3}} \nu^{\frac{2}{3}}, \quad [t] = (2Ag)^{-\frac{2}{3}} \nu^{\frac{1}{3}};$$

the results are presented in the same units. We use elements of size 30^3 with 12 collocation points in each direction, which is equivalent to the spectral resolution with $\Delta = 3$. The size of our computational domain is $1920 \times 1920 \times 1440$ physical units, or $768 \times 768 \times 576$ collocation points. We stop our simulation at time, $t = 128$, when the width of the mixing layer reaches the domain size. At the end of simulation, the Reynolds number reached $\mathfrak{R} = 7500$ to $\mathfrak{R} = 13000$ depending on the initial conditions, where $\mathfrak{R} = \frac{4h\bar{h}}{\nu}$. For comparison, the largest Rayleigh-Taylor simulation to date [12] was performed in a 3096^3 domain at resolution $\Delta = 1$ and reaching time $t = 248$ and $\mathfrak{R} = 30000$. Our relatively coarse resolution might raise concerns, especially in diagnostics of small structures. Nevertheless, all our results, including the spectra and the estimates for microscale η , are in a very good agreement with [12], as well as with our finer-resolved (but smaller) simulation with $\Delta = 1$.

The boundary conditions are periodic in the horizontal directions and no-slip in vertical direction. The initial conditions include a quiescent velocity and a slightly perturbed interface between the layers, $c(t = 0; z) = -\theta(z + \delta(x, y))$, where $\theta(z) = \frac{1}{2}[1 - \tanh(0.4z)]$ is the function describing the density profile across the interface and $\delta(x, y)$ is the perturbation.

We consider simulations with two types of initial perturbation: (1) a narrow initial spectrum, with modes $36 \leq n \leq 48$ and spectral index 0; and (2) a broad initial spectrum [21], with modes $6 \leq n \leq 96$ and spectral index -1. Here the spectral index refers to the exponent of the wavenumber, as in [17], and describes the shapes of the spectra. In both cases, the (initial) fastest growing mode is located at $n \approx 80$ ($\lambda \approx 24$). The two regimes were identified in previous studies as giving distinctly different $h(t)$ at transient times [17]. According to [17], the first system develops a mode-merging regime and exhibits scalings with universal α , while the second system develops in the regime of mode-competition, with α depending on the amplitude of the initial perturbation.

One important focus of our simulations/analysis is on resolving the vertical inhomogeneity of the mixing zone (Figure 1). To achieve this goal we differentiate vertical slices within a given snapshot, thus calculating various characteristics of the mixing zone such as the energy containing scale, the energy spectra and the viscous scale. We collect statistics within a given slice z , e.g. contrasting results for the mixing zone center and its periphery.

II. SCALES OF RAYLEIGH-TAYLOR TURBULENCE

A. Mixing zone width

The mixing zone width is the standard characteristic used in α -studies [6]. According to the most recent analysis [11, 12], the mixing zone width obeys the scaling, $\sqrt{h} = \sqrt{h_0} + t\sqrt{\alpha Ag}$, where h_0 is an initial-conditions-

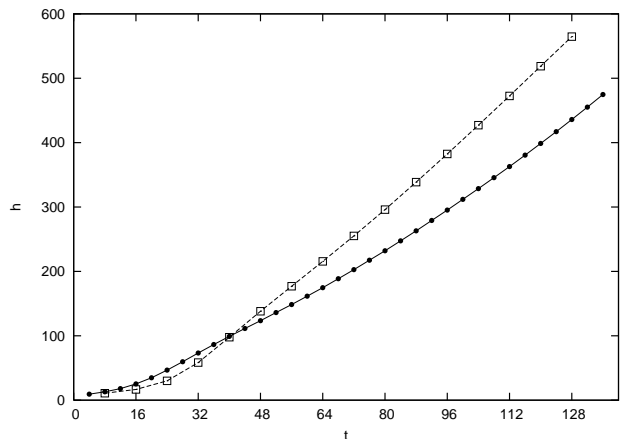


FIG. 2: Mixing widths h in simulations with narrow (solid line) and wide (dashed line) initial spectra.

dependent constant. In the simulation with narrow initial spectrum, we reproduce this scaling relatively well; in the faster-developing simulation with a broad initial spectrum the scaling is affected by the finite domain size (Figure 2).

The value of α depends on the definition of the mixing zone width. Following [7, 12] we consider the definition of the mixing zone width based on the so-called mixing function $M(c) = 4c(1 - c)$

$$h = \int M(\bar{c})dz, \quad (3)$$

where bar denoted averaging over the horizontal plane. We prefer integral definitions of the mixing zone width over the common definitions based on the values of \bar{c} (for example the half-distance H between two heights where $\bar{c} = 0.01$ and $\bar{c} = 0.99$) simply due to the fact that integral quantities are less sensitive to the profile of $\bar{c}(z)$ at the edges of the mixing layer, and consequently less sensitive to the size of computational domain. In the established self-similar regime unrestricted by domain boundaries, two definitions of the mixing zone width are actually within an $O(1)$ systematic factor of each other. The value of the coefficient α , determined from the slopes of the curves shown in Figure 2 at $t > 60$ are $\alpha = 0.029$ for the narrow initial spectrum and $\alpha = 0.040$ for the broad initial spectrum.

An important thesis of the phenomenology [13] is that the internal structure of the mixing zone senses the overall time scale only adiabatically through slowly evolving large scale characteristics, of which the mixing zone width, h , is the most popular one. Therefore, our intention is to separate the “large scale” question of the overall time dependence of the mixing zone width from the set of focused “small scale” questions about internal structure of the mixing zone. To achieve this goal, we track the dependence of the various internal characteristics of the mixing zone (see below) on the mixing zone width.

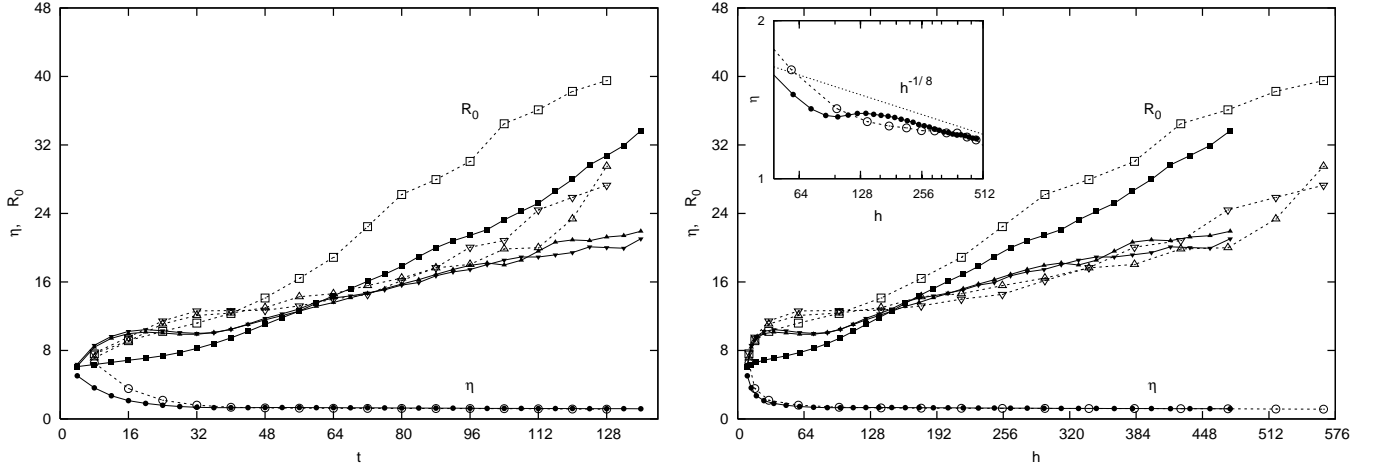


FIG. 3: The energy containing scale (correlation length) and the viscous scale in the middle of mixing layer in the simulations with narrow (solid line) and broad (dashed line) initial spectra. Squares and triangles correspond to scales computed using vertical and horizontal components of the velocity, respectively.

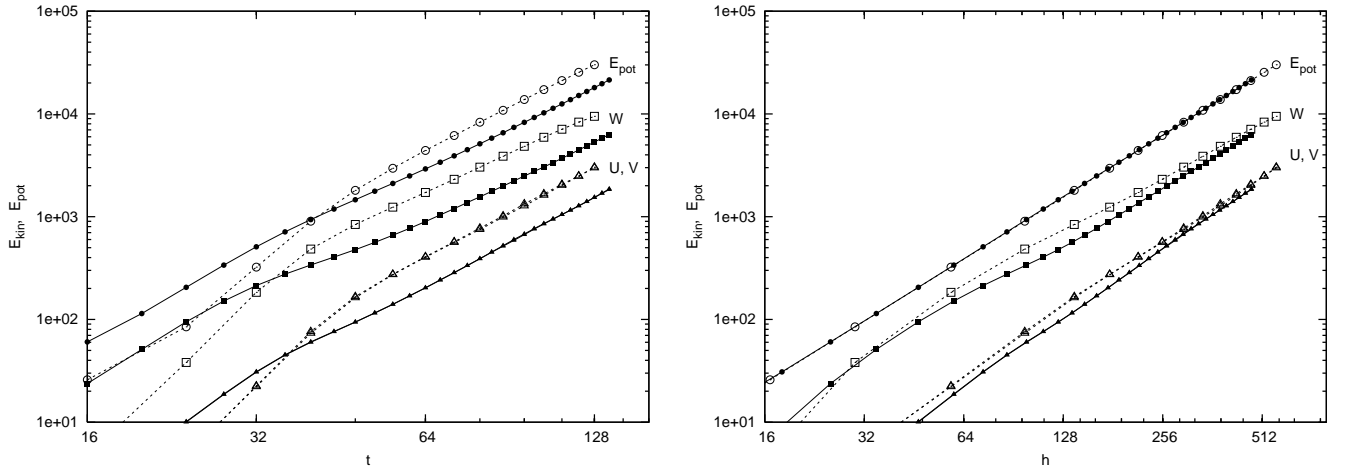


FIG. 4: Released potential energy and components of the kinetic energy integrated across the mixing layer in simulations with narrow (solid line) and broad (dashed line) initial spectra.

B. Energy-containing scale

The energy-containing scale represents a typical size of a turbulent eddy which, intuitively, corresponds to a size of the large scale vortices seen in the mixing zone snapshot, e.g. shown in Figure 1. Formally, it is convenient to define this scale, R_0 , as the correlation length of the normalized two-point pair correlation function of velocity, $f(R) = \langle v_i(r)v_i(r+R) \rangle / \langle v_i^2 \rangle$, where v_i is a selected spatial component of velocity \mathbf{v} . We estimate R_0 as a half width of the correlation function, $f(0)/f(R_0) = 2$. R_0 , defined this way, is consistent (up to some π -dependent constant) with the wavelength (inverse of the wave vector) at which the turbulent energy spectra achieves its maximum. See e.g. Figure 7.

In the developed regime, the correlation length taken at the center of the mixing zone grows linearly with the

mixing layer width, $R_0 \approx h/30 + 7$ and $R_0 \approx h/17 + 6$ for correlations between horizontal and vertical velocities respectively for both types of initial perturbation (Figure 3). In the limit of large R_0 , this suggests significant separation between the two scales, $h : R_0 = 17 : 1$ or more.

Ristorcelli and Clark [11] introduced their version of the energy containing scale as $L = v_z^3/\epsilon$, and found this scale to be of the order of the width of the mixing layer, $L \approx 0.4h$. Note that defining L requires a single point measurement, while R_0 characterizes the two-point correlations. This single-point nature of L makes it the preferred large scale characteristic in the engineering closure modeling. Our simulations show that L is significantly larger than R_0 , where both L and R_0 scales linearly with h : $L \approx 7 - 15R_0 \approx 0.5h$. The scale separation of L and R_0 may be viewed as a very favorable fact for the

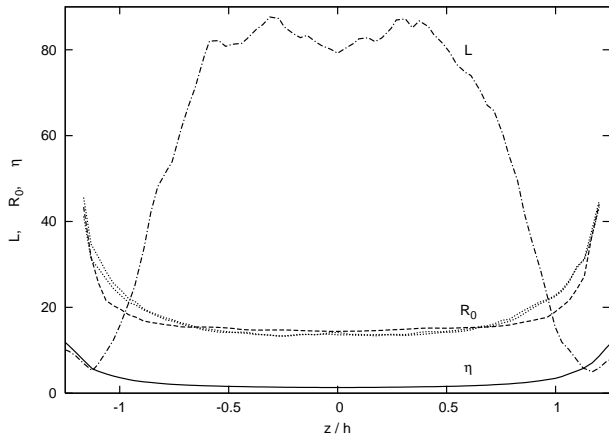


FIG. 5: The energy containing scale based on the two-point correlations, R_0 , and based on the single point measurements, L , and the viscous scale, η , plotted as functions of the distance from the middle of the mixing layer at time $t = 64$ in simulations with narrow initial spectrum. Dashed and dotted lines correspond to scale R_0 computed using vertical and horizontal components of velocity respectively.

engineering modeling of the RTT, thus suggesting a numerical justification for the closure schemes, e.g. of the type discussed in [11].

C. Viscous and dissipation scales

In our simulations $\kappa = \nu$, thus the viscous and dissipation scales are equal to each other.

We estimate the viscous scale in the middle of the mixing layer ($z = 0$) directly as $\eta \sim (\nu^3/\epsilon)^{1/4} \sim (\nu^2/\langle 5(\nabla v)^2 \rangle)^{1/4}$. (The "5"-factor here is due to a turbulence phenomenology tradition, see e.g. [19].) In magnitude, the viscous scale agrees with [12] and with the respective phenomenology estimate [11, 13], $\eta \sim ((\nu/v)^3 h)^{1/4}$. The viscous scale decreases slowly with time (see Figure 3). However, our data are too noisy to claim anything more than rough consistency with the $h^{-1/8}$ predicted in [11, 13] and observed in [11, 12].

D. Relative dependence of scales

In view of our focus on the internal structure of the mixing zone, we choose to study the relative dependence of the relevant scales. Thus, Figure 5 shows dependence of the energy-containing and viscous scales on the mixing zone width.

Analyzing simulations of RTT corresponding to different initial perturbations, we confirm the earlier observed [10, 11] sensitivity of time-evolution of the mixing zone width, scales η and R_0 , and the integral quantities to initial conditions. (See left panels in Figures 3 and 4.) However, we also find that the same quantities re-plotted

as functions of h look very much alike (Figures 3 and 4, right panels). Therefore, one conclusion we draw here is that the relative scale representation is actually a better indicator of turbulence within the mixing zone.

III. STRUCTURE OF THE MIXING LAYER

A. Self-similarity

Figure 6 shows the mixing function and the RMS-averaged velocities across the mixing layer as functions of height, z . In magnitude, the velocities are scaled by $h^{1/2}$, as suggested by the h^2 -dependence of the total kinetic energy: $E \sim v^2 h$ (See Figure 4). The curves taken at three different times are almost indistinguishable from each other. Therefore, one concludes that the mixing zone, viewed from the large-scale perspectives, is self-similar. These observations are in agreement with previous reports [9, 11]. The h -scaling and self-similarity of mean profiles are also observed in the probability distribution functions and in the correlation functions for density and velocities, computed at $z = 0$.

Figures 6 show (in addition to the mixing function) the quantity $\theta(z) = 1 - \overline{M(c)}/M(\bar{c})$ which appears almost constant inside of the mixing layer, with sharp drop-off near the edges. This suggests that a θ -based definition of the mixing zone width can be advantageous, generating a more robust scaling.

B. Dependence of scales on z -location

We found, and the results are shown in Figure 5, that the energy containing scale R_0 and the dissipation scale η exhibit monotonic dependence on z/h . Both scales vary insignificantly across the mixing layer with a slight increase toward the edges.

Comparing the respective curves for different initial spectra, we find that dependence of $R_0(z/h)$ and $\eta(z/h)$ on initial perturbation is weak.

C. Energy spectra

As expected, with the development of the instability, the level of fluctuations grows with time and thus the spectral maximum of the turbulence spectra moves towards larger wavelengths. The energy-containing wavelength, λ_0 , is in agreement with the correlation radius, R_0 . For example, the maximum of the W^2 -spectrum obtained at $z = 0$ and $t = 64$, and shown in Figure 7 (right), is located at $k \approx 0.15$, i.e. $\lambda \approx 42$. The correlation radius at this time is $R_0 \approx 14 \sim \lambda/\pi\sqrt{2}$. At time $t = 124$ the spectrum maximum shifts to $k = 0.07$ ($\lambda \approx 90$) while $R_0 \approx 30$.

Extracting from the spectral data, of the type shown in Figure 7, Kolmogorov scaling for velocity fluctuations at

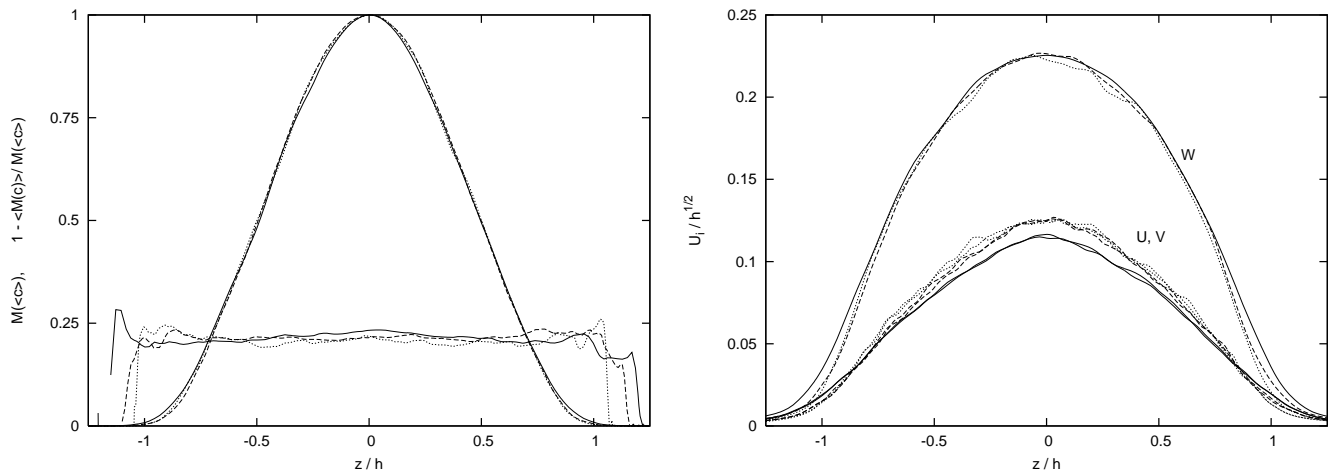


FIG. 6: Mixing function (top) and velocities (bottom) as function of the distance from the center of the mixing layer. The quantities are shown at times $t = 64$ (solid line), $t = 96$ (dashed line), and $t = 128$ (dotted line) for narrow initial spectrum.

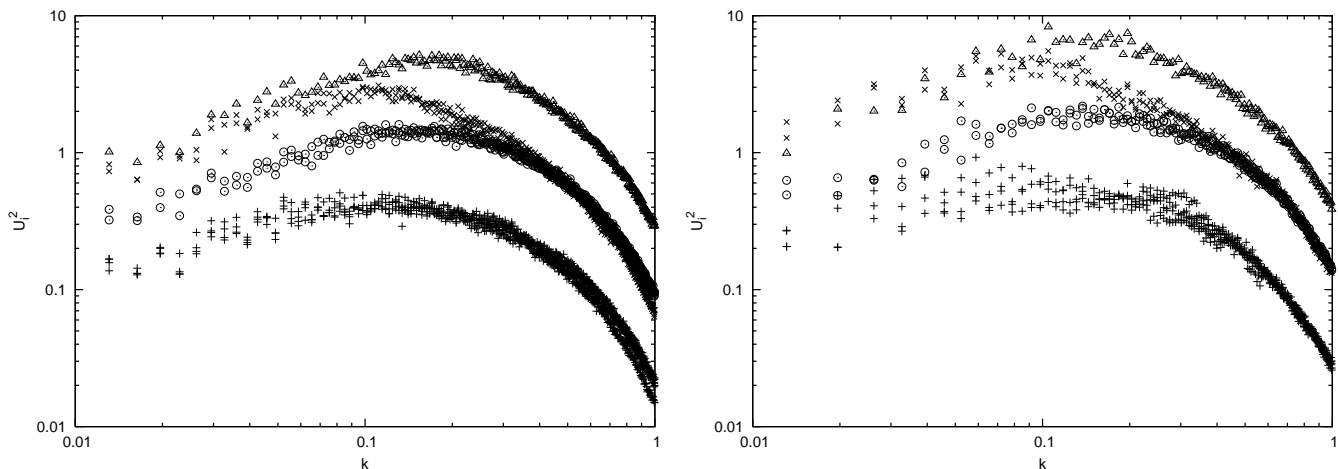


FIG. 7: Energy spectra at time $h \approx 180$ in horizontal planes $z = 0$ (circles - horizontal velocities, triangles - vertical velocities) and $z \pm 0.75h$ (+ horizontal velocities, x vertical velocities) in simulations with narrow (left) and broad (right) initial spectra.

different wavelengths (scales) as well as the largest wavelength cutoff (correspondent to inverse viscous scale) is problematic due to the lack of spatial resolution. Based on our simulation results, we can only state that the range of scales compatible with the Kolmogorov scaling grows with time and the viscous scale decreases with time in accordance with the predictions of [11, 13].

Our simulations suggest that turbulence spectra, shown in Figure 7 for different z -slices within a given snapshot, evolve monotonically with z/h . In other words, all the characteristics of the turbulent spectra, e.g. energy containing scale, viscous scale and the level of fluctuations, estimated in the mixing zone center and at a z -slice close to the mixing zone periphery are parametrically equivalent and one does not observe any qualitatively new behavior at an off-centered slice in comparison with the mixing zone center.

IV. CONCLUSIONS

We conclude by presenting a question-answer style summary for the observations made in the manuscript.

- *Does the relative dependence of the characteristic scales constitute a better indicator of self-similarity within the RTT than respective dependence of the individual scales on time?* We found that the energy-containing scale, R_0 , and the viscous scale, η , exhibit monotonic evolution with h . At transient times both R_0 and η demonstrate much cleaner scaling with h than with the observation time t .
- *How does the energy containing scale, R_0 , compare with h ?* We found that at late time, the ratio of R_0 to h taken at the center of the mixing zone is $\approx 1 : 20$ kept steady in time.

- *Do the turbulent spectra vary with vertical position of the mixing zone?* Analyzing spatial correlations for a given time snapshot we did not observe any qualitatively new features of the turbulence spectra with transition from the vertically central slice to an off-centered one within the mixing zone.
- *How different are the scales and the spectra corresponding to qualitatively different initial perturbations?* We found that the dependencies of R_0 and η , as functions of z/h , on the initial perturbations are weak.

Our immediate further plan is to extend this type of analysis to account for effects of chemical reactions on

the RT Boussinesq turbulence.

Acknowledgments

We wish to thank P. Fischer for the permission to use the Nekton code, A. Obabko and P. Fischer for the detailed help in using the code, and J.R. Ristorcelli for useful comments. This work was supported by the U.S. Department of Energy at Los Alamos National Laboratory under Contract No. DE-AC52-06NA25396 and under Grant No. B341495 to the Center for Astrophysical Thermonuclear Flashes at the University of Chicago.

-
- [1] Rayleigh, Lord, *Investigation of the character of the equilibrium on an incompressible heavy fluid of variable density*, Proc. of the London Math. Soc. **14**, 170 (1883).
 - [2] G. Taylor, Taylor, Sir Geoffrey Ingram, *The instability of liquid surfaces when accelerated in a direction perpendicular to their planes*, Proc. of the Royal Soc. of London. Series A, Mathematical and Physical Sciences, **A201**, No. 1065, 192 - 196 (1950).
 - [3] S. Chandrasekhar, "Hydrodynamic and hydrodynamic instability", Dover Publications, NY 1961.
 - [4] R.E. Duff, F.H. Harlow, C.W. Hirt, *Effects of diffusion on interface instability between gases*, Phys. Fluids **5**, 417 (1962).
 - [5] D.H. Sharp, *An overview of Rayleigh-Taylor instability*, Physica D **12**, 3 (1984).
 - [6] G. Dimonte et al, *A comparative study of the turbulent Rayleigh-Taylor instability using high-resolution three-dimensional numerical simulations: The Alpha-Group collaboration*, Phys.Fluids **16**, 1668 (2004).
 - [7] S.B. Dalziel, P.F. Linden, D.L. Youngs, *Self-similarity and internal structure of turbulence induced by Rayleigh-Taylor instability*, JFM **399**, 1 (1999).
 - [8] P.N. Wilson, M.J. Andrews, *Spectral measurements of Rayleigh-Taylor mixing at small Atwood number*, Phys. Fluids **14**, 938 (2002).
 - [9] Y.N. Young, H. Tufo, A. Dubey, R. Rosner, *On the miscible Rayleigh-Taylor instability: two and three dimensions*, JFM **447**, 377 (2001).
 - [10] A.W. Cook, P.E. Dimotakis, *Transition stages of Rayleigh-Taylor instability between miscible fluids*, JFM **443**, 69 (2001).
 - [11] J.R. Ristorcelli, T.T. Clark, *Rayleigh Taylor turbulence: self-similar analysis and direct numerical simulation*, J. Fluid. Mech. **507**, 213 (2004).
 - [12] W.H. Cabot, A.W. Cook, *Reynolds number effects on Rayleigh-Taylor instability with possible implications for type Ia-supernovae*, Nature Physics **2**, 562 (2006).
 - [13] M. Chertkov, *Phenomenology of Rayleigh-Taylor Turbulence*, Phys.Rev.Lett. **91**, 115001-4 (2003).
 - [14] A.N. Kolmogorov, *The equation of turbulent motion in an incompressible viscous fluid*, Izv.Akad. Nauk. SSSR, Ser.Fiz. **VI**(1-2), 56 (1941).
 - [15] A. Celani, A. Mazzino, L. Vozella, *Rayleigh-Taylor turbulence in two dimensions*, Phys.Rev.Lett. **96**, 134504/1-4 (2006).
 - [16] M. Zingale et al, *Three-dimensional numerical simulations of Rayleigh-Taylor unstable flames in Type Ia supernovae*, Astrophysical Journal **632**, 1021-34 (2005).
 - [17] P. Ramaprabhu, G. Dimonte, M.J. Andrews, *A numerical study of the influence of initial perturbations on the turbulent Rayleigh-Taylor instability*, J.Fluid.Mech. **536**, 285 (2005).
 - [18] P.F. Fischer, G.W. Kruse, and F. Loth, *Spectral element methods for transitional flows in complex geometries*, J. of Sci. Comput. **17**, 81-98 (2002).
 - [19] H. Tennekes, J.L. Lumley, *First course in turbulence*, MIT Press, 1972.
 - [20] In two dimensions RTT is markedly different from its three dimensional counterpart: buoyancy and inertia effects are in balance, resulting in the so-called Bolgiano-Obukhov scaling regime. The 2d phenomenological prediction of [13] was numerically confirmed in [15].
 - [21] In current preprint, the simulation with a broad initial spectrum was performed in smaller domain of size 960^3 with modes $3 \leq n \leq 96$ and spectral index -1. The larger simulation is on the way.